Proceedings of the ASME 2010 International Design Engineering Technical Conferences & Computers and Information in Engineering Conference
IDETC/CIE 2010
August 15-18, 2010, Montreal, Quebec, Canada

DETC2010-29233

THE INFLUENCE OF POST ANGIOPLASTY STENT IMPLANT PROFILE ON ARTERIAL WALL STRESS

Mircea Teodorescu*
School of Engineering
Cranfield University
Bedford MK43 0BS
Email: m.teodorescu@cranfield.ac.uk

Moshe Brand
Department of Mechanical Engineering and Mechatronics
Faculty of Engineering
Ariel University Center of Samaria
Ariel, Israel
Email: mosheb@ariel.ac.il

Jacob Rosen
Department or Computer Engineering
Baskin School of Engineering
University of California at Santa Cruz
Santa Cruz, CA 95060, USA
Email: rosen@ucsc.edu

Homer Rahnejat
Wolfson School of Mechanical and Manufacturing Engineering
Loughborough University
Loughborough, LE11 3TU, UK
Email: h.rahnejat@lboro.ac.uk

ABSTRACT

One of the main causes for post angioplasty arterial restenosis is the excessive stress induced in the arterial wall during and after the medical intervention. The closed stent is introduced in the artery wrapped around the deflated balloon catheter and is expanded in the final position by inflating the balloon. Unfortunately, this process also stretches the arterial wall. Additionally, for the stent to be successful, its diameter must be slightly larger than the diameter of the inflated artery. The stent is usually a dense mesh of interconnected beams. Therefore, it is often considered that it applies a constant pressure to the artery / stent interface. However, in reality each beam individually presses against the innermost layer of the artery (intima).

The current study proposes a model, which predicts the arterial wall subsurface stress field due to individual stent beams. It was found that the local shape of the contact (beam cross section) plays an important role close to the stent / intima contact. Sharper edged cross sections (e.g. square) promote higher stresses. It was observed that during restenosis a new inner layer (neointima) is formed, significantly reducing the stent efficiency. This could be related to local stress concentrations due to the choice of stent beam profile.

NOMENCLATURE

D $= 0.5 \div 1mm$ – difference between the diameter of the stent and the diameter of the inflated artery [1]
R $= 2.125mm$ – radius of the stent [1]
r $= 55\mu m$ – significant dimension of the beam cross section [1]
l_j distance between adjacent stent beams
l $= l_1 + l_2 = 2\pi R/9$
E_i Elasticity modulus of successive layers of the artery
d_i thickness of successive layers of the artery
P_0 average constant pressure
P_k amplitude of the k^{th} harmonic of the applied pressure
l_{max} maximum depth
x coordinate along the contact surface

*Address all correspondence to this author.

y coordinate into the depth of the contacting solid

u_0 surface deflection

${}_k u_y$ deflection of the solid due to k^{th} harmonic of the applied pressure

ν_i Poisson ratio of successive layers of the artery

${}_k\Omega_y$ generic deflection function [2, 3]

$i \in \{Intima, Media\}$

$j \in \{1, 2\}$

INTRODUCTION

The National Heart Lung and Blood Institute (NHLBI) of the National Institute of Health (NIH) stated that heart disease is the leading cause of death in the USA [4]. In 2010, an estimated 785 000 Americans will have a new coronary attack, 470 000 will have a recurrent attack and an additional 195 000 silent first myocardial infarctions [5]. The cause of many of these incidents is untreated (or recurring) coronary atherosclerosis.

Traditionally, the remedy was either a pathological therapy or a by-pass surgery. While the first could often not be effective enough, the second implies an invasive procedure. The third solution, firstly proposed by Dotter and Judkins in 1964 [6], involves a mesh-like structure (stent), which is implanted in the artery at the specified location. This supports the arterial wall and improves the blood flow (see figure 1). This less-invasive operation (angioplasty) proved a viable alternative and today is the solution of choice in most cases. In 2006, in the USA there were over 1 million angioplasty procedures (more formally known as Percutaneous Coronary Intervention or PCI) [5]. Approximately 76% use drug-eluting stents and only 24% bare-metal stents [5]. However, the challenge of restenosis is looming on for almost all PCI cases [7]. For example, for the drug-eluting stents, the restenosis rate per stent was 3.5% after 1 year and 4.9% after 2 years [8]. Much effort has been expended on developing strategies designed to effectively treat this problem. There are two possible solutions. Firstly, through use of mechanical means such as minimal plaque removal by directional atherectomy, or extensive debulking (rotational atherectomy), to create the largest possible lumen and prevent recoil. Secondly, systemic and local use of numerous drug classes including antithrombotic, antiplatelet, steroids, and other antiinflammatory agents may be made [7].

Although removing the recurring plaque is a relatively successful procedure, it would be ideal to find a method, which would prevent it from occuring in the first place. Because a strong correlation has been observed between the restenosis and stent/artery mechanical interaction, finding a remedy should ideally start with a fundamental analysis of both artery mechanics and stent design. The artery wall consists of a number of successive layers, each with a specific function [9, 10] (see figure 1). The structural strength of the artery is provided by the outer layers: adventitia and media (the latter is a thick layer of smooth muscle cells). These are relatively thick layers, designed to withstand the internal pressure due to blood flow. The innermost layer (Intima) is very thin and soft. This layer is in permanent contact with the blood flow and its main role in a healthy artery is to lower the fluid drag [11]. However, during angioplasty operation this layer can be damaged. This damage is partly due to the passing self-expandable ballon-like structure (which brings and leaves the stent in place) [12] and partly by the interaction between the stent and the wall. It is generally accepted that the second interaction is responsible for most of the damage. Numerous studies have modeled the arterial wall properties and the wall/stent interaction, using either a fully numerical approach (e.g. Finite Element Method: FEM) [10, 13–15], an analytic representation of the stent [16, 17], or a mixture of both methods. However, in the latter case, the contact between the stent and the artery is usually modeled using FEM [13].

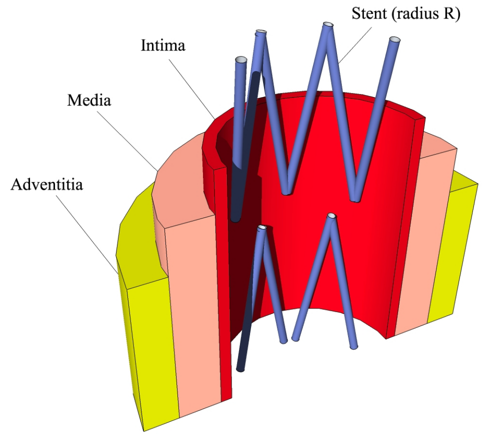

FIGURE 1. GENERIC VIEW OF THE STENT MOUNTED IN THE ARTERY

The main challenge for modelling the problem is the multidisciplinary nature of it. This includes transient fluid mechanics (pulsatile incompressible blood flow [11]), highly nonlinear arterial mechanics (including all the successive layers), stent elastoplastic mechanics and contact mechanics between the stent and the artery. Unfortunately, such a solution is not only very difficult, but almost impossible with the currently available computational algorithms. Therefore, each research group confines its investigation to a limited set of features at a time.

One aspect of the problem which has received less attention than others is the contact interaction between the stent and the artery. Although many research groups have considered this interaction, in most cases the predictions are made using an averaging method (e.g. FEM). This can predict the general picture and give valuable information regarding the stress level in the arterial wall (mainly due to stretching). However, the methods used cannot predict the localised contact stresses. If the experimental observations (that the plaque is formed due to mechanical interaction between stent and artery wall) are valid, a detailed study of the contact interaction must be conducted.

The current paper predicts the local deformation of the arterial wall as well as the induced subsurface stress field during the stent-artery interaction. Several possible stent beam cross-sections and contact conditions are considered. This study is a first stepping stone in making detailed contact predictions. The "Results and Discussions" section (e.g. Figures 8 and 9) shows good approximation of the real phenomena.

MATHEMATICAL MODEL

The arterial wall represents a succession of concentrical soft-tissue layers, each of which with its own structure and mechanical properties [9]. The stent, which is an interconnected frame of thin beams pushes the innermost layer and therefore, stretches the wall through Poisson effect. To achieve a permanent bond between the stent and the artery, the stent diameter must be slightly larger than the arterial internal diameter. If the stent diameter is too large the artery could be damaged. However, if the diameter is too small, the stent can separate from the artery. Brand *et al.* [16, 18] calculate the average stress in the arterial wall and define a dimensionless parameter (DF = Damage Factor). This is the ratio between the average stress on the arterial wall and average blood pressure (100mmHg). The prediction was considered for diametral mismatch of up to 1mm.

The current study uses similar geometrical configuration (and diametral mismatch) and investigates the localised effects of the stent-beam/arterial-wall interaction. Figure 2 shows a schematic representation of the cross section through the stent-artery wall contact. In the current example, the stent is made of successive rings (chains) of angled beams [16, 18]. Each chain has 18 beams (segments), which are coupled at their corners (see figure 1). Considering the tissue to be very soft in comparison with the stent material, as the first assumption the beams are assumed to remain parallel. Therefore, the problem can be simplified to a plane strain rigid punch in terms of contact mechanics problems [19]. The distance between adjacent beams is $l_{1,2}$ (see figure 2), where for an 18 beam configuration $l = l_1 + l_2 = 2\pi R/9$.

The beam cross section is the result of stent manufacturing technique. There are two possible cases; rectangular or circular cross sections. The first one is used more, because the stent can be easily cut from a thin circular tube. The scope of the current paper is to understand the implications of the geometrical shape and the physical interaction between the beam and the wall. Therefore, the advantages and disadvantages of each of the profiles can be ascertained.

Depending on the loading characteristics, each layer can sustain (perfectly) elastic, viscoelastic or stress softening behav-

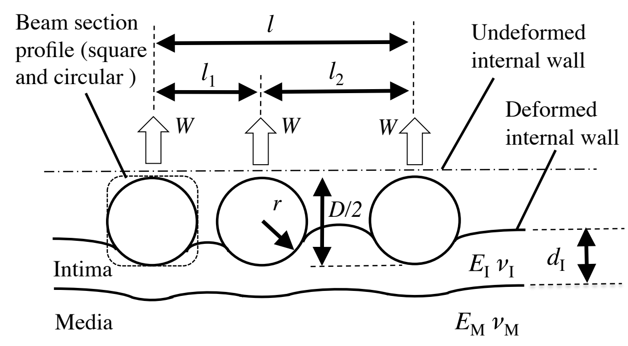

FIGURE 2. CONTACT BETWEEN THE STENT AND THE MULTY-LAYERED ARTERY WALL

ior [9]. Therefore, modeling the behaviour of a succession of layers is probably the most challenging, given the physical characteristics of the arterial wall. The stent beam considered for the current study has a square section and a very small cross section ($110 \times 110\mu m$ [16,18]). Consequently, it is expected to have high stress concentration very close to the stent/wall interface. To understand stress propagation through intima and inner region of media, it is a good 1st approximation to consider that both have a purely elastic behaviour. Therefore, the problem simplifies to a rigid punch indenting a single bonded layer in contact mechanics terms. For the numerical case, it was considered that the intima is a thin and soft ($d_1 = 10\mu$m and $E_I = 1$MPa) layer, bonded on a harder substrate ($E_2 = 3$MPa) [20].

The contact mechanics model proposed by Teodorescu *et al.* [2, 3] was carefully adopted. This method decomposes the contact pressure distribution into a series of harmonic waves and predicts the subsurface stress and strain fields for each harmonic. If the contact pressure distribution is expressed as:

$$p(x) = \frac{1}{2}P_0 + \sum_{k=1}^{N\to\infty} P_k \cos(\alpha_k x - \phi_k) \tag{1}$$

The subsurface stress and strain fields are:

$$\begin{cases} \sigma_{ij}^{\xi} = {}_0\sigma_{ij}^{\xi} + \sum_{k=1}^{N\to\infty} {}_k\sigma_{ij}^{\xi} \\ \varepsilon_{ij}^{\xi} = {}_0\varepsilon_{ij}^{\xi} + \sum_{k=1}^{N\to\infty} {}_k\sigma_{ij}^{\xi} \end{cases} \tag{2}$$

where $i, j \in \{x, y\}$ and $\xi \in \{\text{Intima, Media}\}$

The k^{th} component of the subsurface deflection is:

$${}_k u_y = \int_y^{l_m ax} {}_k\varepsilon_y dy \tag{3}$$

and the total contact and subsurface deflection is:

$$u_y = {}_0u_y + \sum_{k=1}^{N\to\infty} {}_ku_y \tag{4}$$

where ${}_0u_y$ is the deflection due to P_0, l_{max} is the maximum depth. It should be noted that the surface deflection (at $y = 0$) is u_0.

The advantage of this techniques is the direct link between the applied pressure and the resulting deformation for each harmonic. It was shown [2, 3] that the surface (contact) and subsurface deformation can be expressed as:

$${}_ku_y = \cos(\alpha_k x - \phi_k)\frac{P_k}{E^{\text{Media}}}{}_k\Omega_y \tag{5}$$

where ${}_k\Omega_y$ is a generic deflection function, which contains the material parameters of both, the protective layer and the substrate [2, 3].

In the first instance neither the shape of the contact nor the contact pressures are known. However, the algorithm assumes that there is no physical penetration between the indenter and the deformed material (intima). Therefore, using this physical constraint, both the pressure and local deformation can be computed using an algorithm, which minimises the error and corrects (relaxes) the pressure distribution to avoid physical penetration.

For the current application, the contact loading is provided by the prescribed indentation. In figure 2, D is the diameter mismatch between the stent and the artery. Therefore, the rigid indentation is equal with the radial mismatch: $D/2$. However, if this is applied to an individual beam against a soft base, it would certainly generate an erroneous result. Adjacent beams also work together and the total deformation is as the result of load applied by them all. To simulate this phenomena, in the current analysis, 3 adjacent beams were considered to indent the soft base simultaneously. However, the control beam is considered to be the central one.

RESULTS AND DISCUSSIONS

To understand the full benefit of the protective intima layer, as well as the possible modeling errors if this would be neglected, in the first instance it was assumed that the intima is not present. Therefore, the stent is in direct contact with the arterial wall. Figure 3 a) and figure 4 a) predict the contact pressure and the deformed contact shape for rectangular and circular shaped beams. Figure 3 b) and figure 4 b) show the subsurface stress fields. It can be noted that the sharp corners of the rectangular beam

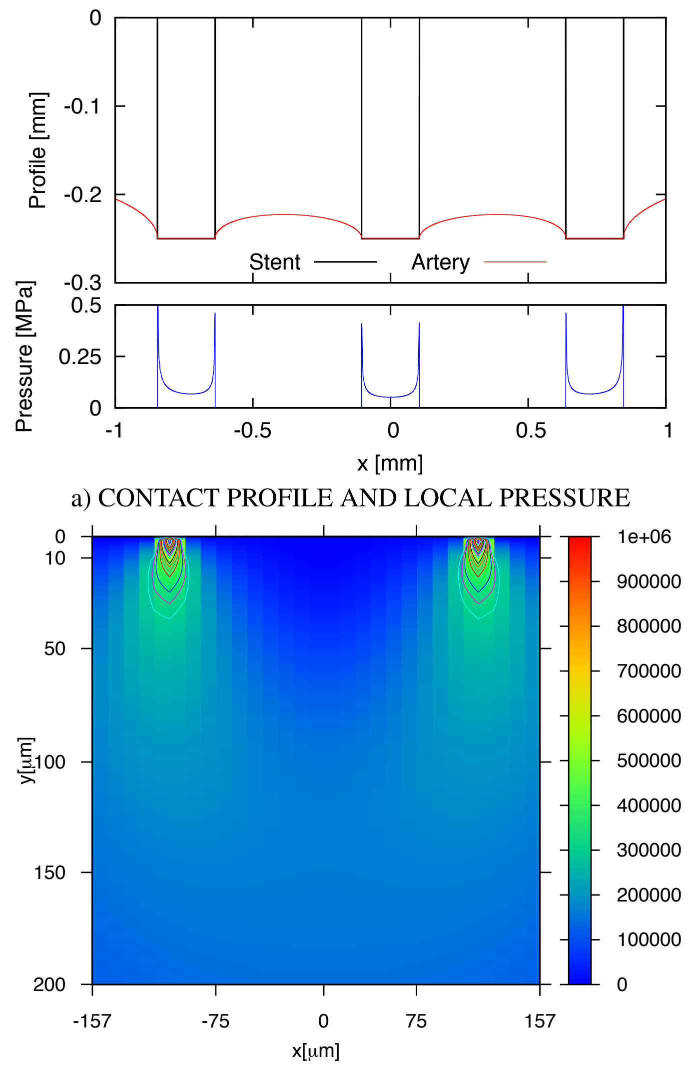

a) CONTACT PROFILE AND LOCAL PRESSURE

b) PRINCIPAL SHEAR STRESS FIELD

FIGURE 3. CONTACT CHARACTERISTICS FOR A STENT WITH RECTANGULAR BEAM SECTION ($D = 0.5$mm)

section lead to high pressure spikes, not unlike those noted for any unprofiled indenter, penetrating a semi-infinite elastic solid . These pressure spikes induce high subsurface stresses very close to the surface. If there is a link between the plaque deposition and arterial wall damage, this stress distribution would certainly have an unfavourable effect.

By including the soft intima layer in the simulation, the stress pattern changes significantly. Figure 5 shows the subsurface stress field for both cases. Firstly, it can be noted that the magnitude of the stress field is much reduced. This is expected because the soft layer (although very thin) deforms under load and it passes the maximum stresses to the substrate beneath it.

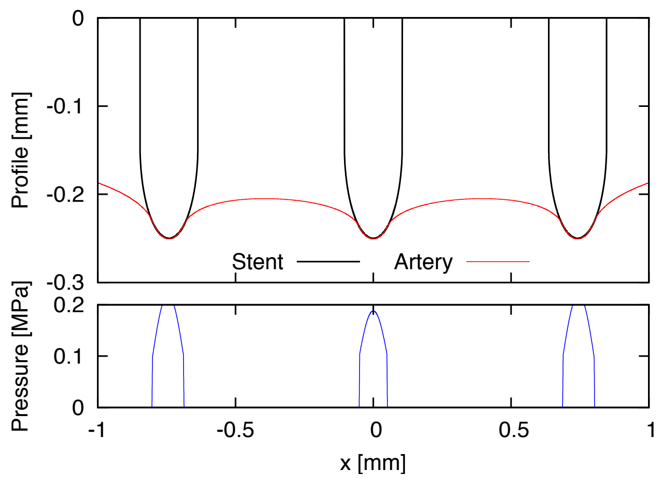

a) CONTACT PROFILE AND LOCAL PRESSURE

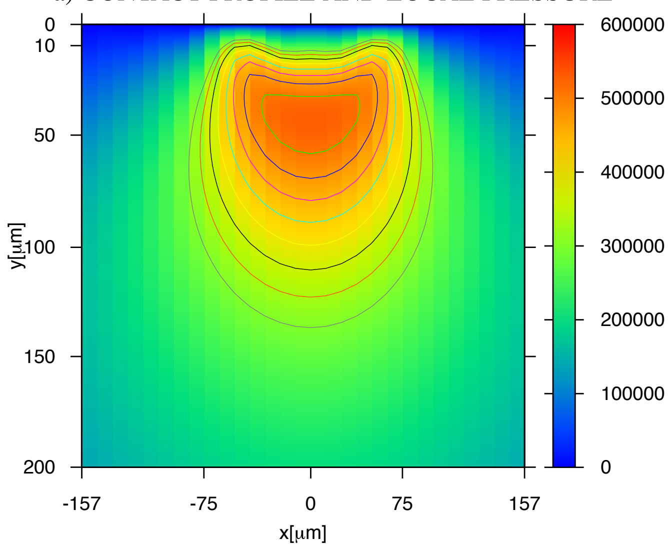

b) PRINCIPAL SHEAR STRESS FIELD

FIGURE 4. CONTACT CHARACTERISTICS FOR A STENT WITH CIRCULAR BEAM SECTION ($D = 0.5$mm)

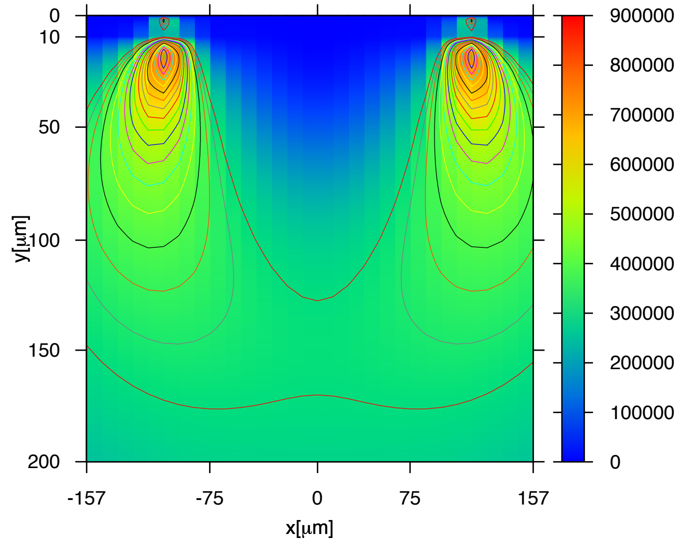

b) RECTANGULAR SECTION

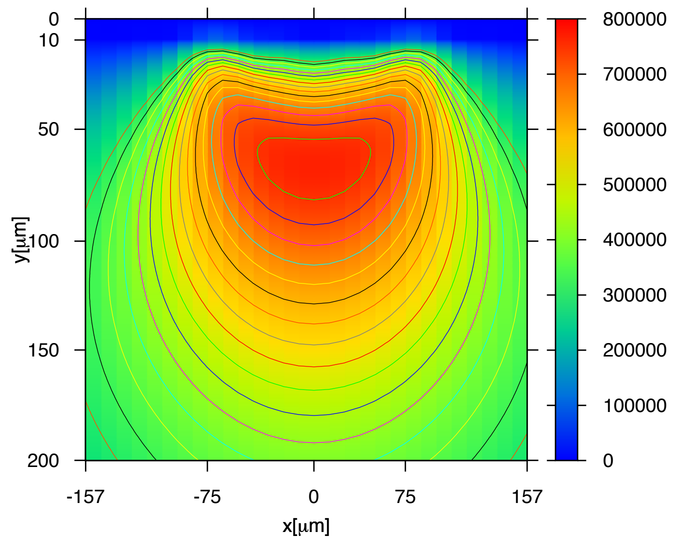

a) CIRCULAR SECTION

FIGURE 5. PRINCIPAL SHEAR STRESS FIELD ($d_1 = 10\mu$m AND $2D = 1$mm)

However, it must also be noted that the mechanism, which leads to a lower stress field is different for the two contact configurations. For the circular cross-section the size of the contact footprint depends on the modulus of elasticity and the magnitude of contact force. The softer superficial layer spreads the effective contact footprint over a slightly larger area, effectively lowering the maximum pressure, and consequently, the maximum shear stresses. In contrast, for the rectangular cross- section, the contact footprint is predefined.

Teodorescu *et al.* [2] showed that the higher the order of the pressure harmonic, the shallower the penetration. Therefore, the effect of higher harmonics stops close to the surface. If the protective layer is worn away, the result is high stresses adjacent to the surface. However, if there is a soft protective layer, this effectively dampens the influence of higher harmonics, which are not passed onto the substrate. Therefore, if the layer is in place, the stress field is significantly diminished and the difference in the maximum subsurface stresses is much less. It must, however, be noted that while for the circular section the maximum stresses are relatively deep below the surface, for the rectangular cross section these are very close to the media/intima interface. Additionally, there are two small islands of high stress embedded in

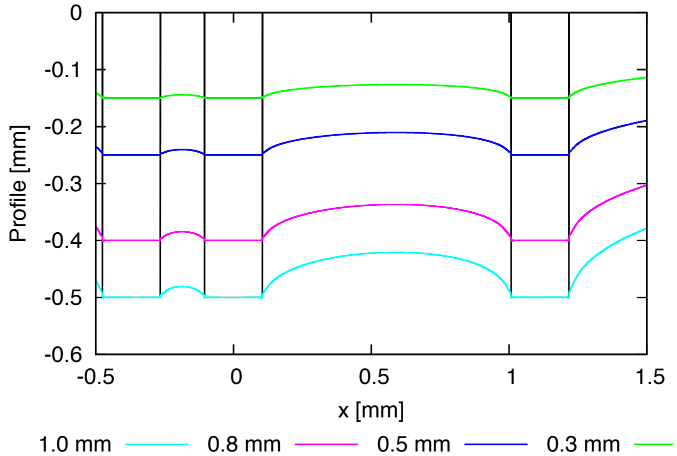

a) CONTACT PROFILE

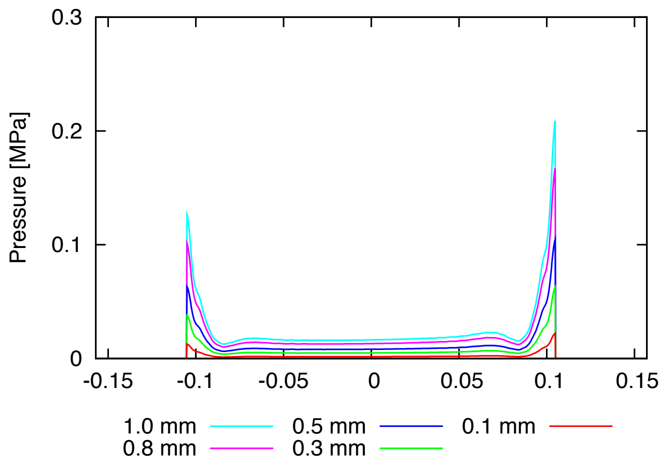

b) CONTACT PRESSURE

FIGURE 6. CONTACT CHARACTERISTICS FOR $l_1 = l/4$, $d_1 = 10\mu$m AND $D = 0.3$mm $\rightarrow$ 1mm

the intima. It is not immediately clear how much these would affect the development of plaque, but one may surmise that they can cause cell failure. Therefore, they can further weaken the arterial wall.

The stent global geometry (number and length of beams in each ring, etc.) affects the overall operation of the device [1]. In the current example it was assumed that the stent has successive rings of 18 interconnected beams. Therefore, the distance between adjacent beams ($l_{1,2}$) varies along the axis of the stent. The stress pattern in figure 5 assumes a perfectly centred beam. However, this is the case only for the central cross-section of the stent. If the stent area under investigation moves away from this central position, the central beam is offset and the distance between it and its neighbours progressively increases or decreases.

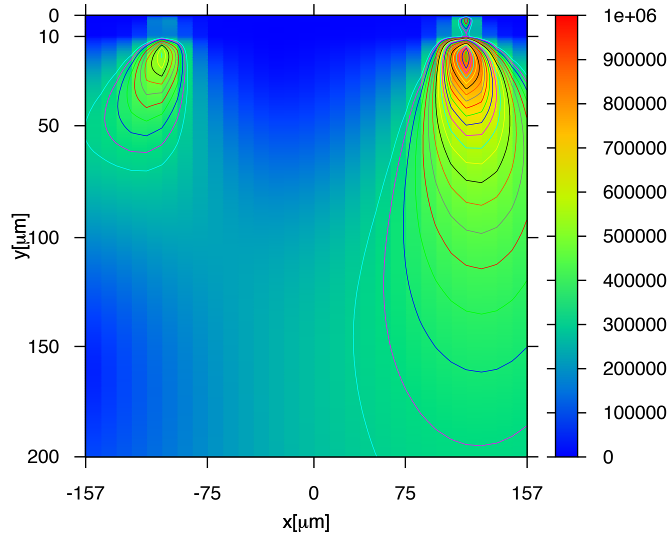

FIGURE 7. SUBSURFACE STRESS FIELD FOR THE CENTRAL BEAM ($l_1 = l/4$, $d_1 = 10\mu$m AND $D = 1$mm)

Figure 6 a) shows the contact profile and pressure if the central beam is eccentrically located ($l_1 = l/4$). It is noted that the increased distance between two adjacent beams can lead to higher contact edge pressure peaks on one side only. This becomes more significant if the diametral mismatch were to increase. Figure 7 shows the subsurface stress field for $l_1 = l/4$ and $D = 1$mm. For this case the field is non-symmetrical, with a very high value, corresponding to the high pressure spike.

To improve the design of the stent and potentially reduce the chance of restenosis, the importance of geometry related stress concentration should be better understood. Figure 8 shows the maximum shear stresses and their location for circular and rectangular beam sections. The first observation is that at small diametral mismatch the circular beam results in higher subsurface stresses than the rectangular section, while at high diametral mismatch the reverse of this trend is true (figure 8 a). However, for a full understanding of the problem, this values must be correlated with the location of the maximum stress. While for the circular cross section (see figure 8 b) an increasing load leads to progressively deeper location of the maximum shear stress (away from the contact), for the rectangular shape the maximum value of the stress remains always very close to the intima/media interface. This observation could have important consequences for the location and magnitude of plaque build-up.

Figure 9 shows the maximum shear stress for different eccentric values of the central beam. For the central location $l_1 = l_2$, while at the end of the beam, where two beams merge, $l_1 = 2r$. In the latter case, the central beam is adjacent to one of its neighboring beams and at the maximum distance from its other neighbor.

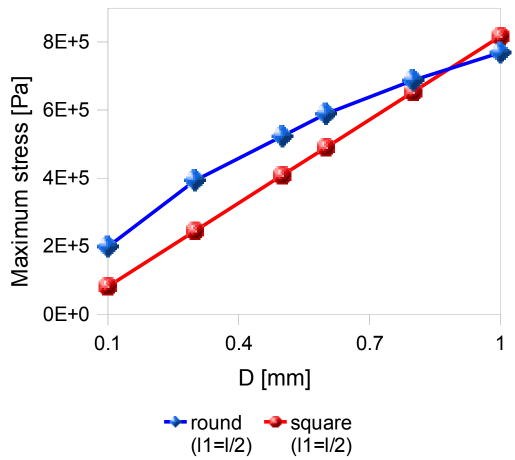

a) MAXIMUM SHEAR STRESSES

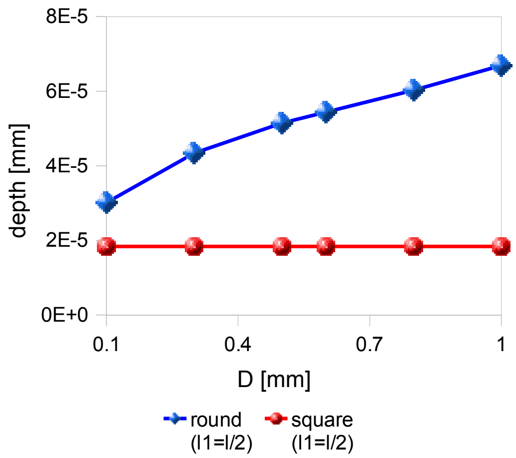

b) DEPTH OF THE MAXIMUM SHEAR STRESSES

FIGURE 8. MAXIMUM SHEAR STRESSES FOR CIRCULAR AND SQUARE SECTIONS ($l_1 = l/2$ AND $d_1 = 10\mu$m)

This represents a major stress concentrator. Therefore it is expected to have the highest subsurface stress.

CONCLUSIONS

The current paper proposes a detailed model for the stent/arterial wall contact mechanics. The contact deformation and subsurface stress field were predicted for two possible stent cross-sections (circular and rectangular). It is concluded that while at small diametral mismatch the rectangular cross-section yields lower subsurface stresses, at high diametral mismatch the situation is reversed. Additionally, the potentially lower stresses predicted for the rectangular cross-section, are located very close to the intima/media interface. This can potentially cause cellular damage and be a contributory source of restenosis.

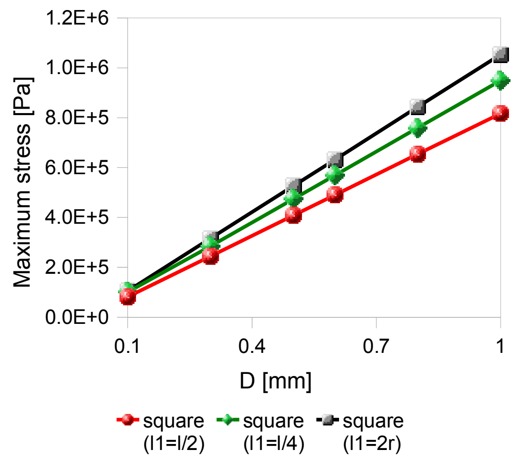

FIGURE 9. MAXIMUM SHEAR STRESSES FOR SQUARE SECTION ($d_1 = 10\mu$m)

REFERENCES

[1] Brand, M., Ryvkin, M., Einav, S., Avrahami, I., Rosen, J., and Teodorescu, M., 2010. "Numerical models of an artery with different stent types". *12^th Mediterranean Conference on Medical and Biological Engineering and Computing – MEDICON 2010, 27 to 30 May 2010 in Porto Carras,Chalkidiki, Greece*.

[2] Teodorescu, M., Rahnejat, H., Gohar, R., and Dowson, D., 2009. "Harmonic decomposition analysis of contact mechanics of bonded layered elastic solids". *Applied Mathematical Modelling,* ***33***(1), pp. 467 – 485.

[3] Teodorescu, M., and Rahnejat, H., 2007. "Mathematical modelling of layered contact mechanics of cam-tappet conjunction". *Applied Mathematical Modelling,* ***31***(11), pp. 2610 – 2627.

[4] NHLBI, 2008. *Disease Statistics. Fact Book Fiscal Year 2008, Chapter 4*. NIH.

[5] Llyod-Jones, D., Adams, R. J., and Brown, T. M., 2010. "Heart disease and stroke statistics 2010 update. a report from the american health association". *Circulation Journal of the American Health Association,* ***121***, pp. 1–171.

[6] Dotter, C. T., and Judkins, M. P., 1964. "Transluminal Treatment of Arteriosclerotic Obstruction: Description of a New Technic and a Preliminary Report of Its Application". *Circulation,* ***30***(5), pp. 654–670.

[7] Simons, M., 2009. "Vegf and restenosis: The rest of the story". *Arteriosclerosis, Thrombosis, and Vascular Biology,* ***29***, pp. 439–440.

[8] Fröbert, O., Lagerqvist, B., Carlsson, J., Lindbäck, J., Stenestrand, U., and James, S., 2009. "Differences in restenosis rate with different drug-eluting stents in patients with and without diabetes mellitusa report from the scaar (swedish

angiography and angioplasty registry)". *Journal of the American College of Cardiology,* ***53 (18)***, pp. 1660–1667.
[9] Holzapfel, G. A., Gasser, T. C., and Ogden, R. W., 2000. "A New Constitutive Framework for Arterial Wall Mechanics and a Comparative Study of Material Models". *Journal of Elasticity,* ***61***(1–3), pp. 1–48.
[10] Hayashi, K., and Imai, Y., 1997. "Tensile property of atheromatous plaque and an analysis of stress in atherosclerotic wall". *Journal of Biomechanics,* ***30***(6), pp. 573 – 579.
[11] Mehdian, M., and Rahnejat, H., 1996. "Blood flow measurement using a highly filled carbon polymer sandwich sensor and an elasto-pseudo compressible vascular flow". *IMechE Part H: Journal of Engineering in Medicine,* ***210***(4), pp. 289–296.
[12] Dunn, A. C., Zaveri, T. D., Keselowsky, B. G., and Sawyer, W. G., 2007. "Macroscopic friction coefficient measurements on living endothelial cells". *Tribology Letters,* ***27***(2), pp. 233–238.
[13] Auricchio, F., Loreto, M. D., and Sacco, E., 2001. "Finite-element analysis of a stenotic artery revascularization through a stent insertion". *Computer Methods in Biomechanics and Biomedical Engineering,* ***4***(3), pp. 249–263.
[14] Holzapfel, G. A., Stadler, M., and Schulze-Bauer, C. A. J., 2002. "A Layer-Specific Three-Dimensional Model for the Simulation of Balloon Angioplasty using Magnetic Resonance Imaging and Mechanical Testing". *Annals of Biomedical Engineering,* ***30***(2), pp. 753–767.
[15] Kiousis, D. E., Gasser, T. C., and Holzapfel, G. A., 2007. "A numerical model to study the interaction of vascular stents with human atherosclerotic lesions". *Annals of Biomedical Engineering,* ***35***(11), pp. 1857–1869.
[16] Brand, M., Ryvkin, M., Einav, S., and Slepyan, L., 2005. "The cardicoil stent-artery interaction". *Journal of Biomechanical Engineering,* ***127***, pp. 337–344.
[17] Brand, M., Ryvkin, M., Einav, S., and Rosen, J., 2009. "Numerical models of an artery with a net structured stent". *WC, IFMBE Proceedings,* ***25***, pp. 1341–1344.
[18] Brand, M., Ryvkin, M., and Einav, S., 2008. "The scimed radius stent-artery interaction". *Proceedings 9 Biennial ASME Conference on Engineering Systems Design and Analysis, July 7-9, Haifa, Israel*.
[19] Johnson, K. L., 1985. *Contact Mechanics*. Cambridge University Press, Cambridge UK.
[20] Laurent, S., Girerd, X., Mourad, J.-J., Lacolley, P., Beck, L., Boutouyrie, P., Mignot, J.-P., and Safar, M., 1994. "Elastic modulus of the radial artery wall material is not increased in patients with essential hypertension". *Arterioscler Thromb Vasc Biol,* ***14***, pp. 1223–1231.